Challenge in Cu-rich CuInSe2 thin film solar cells: Defect caused by etching

Peer-reviewed author version

Elanzeery, Hossam; Melchiorre, Michele; Sood, Mohit; Babbe, Finn; Werner, Florian; BRAMMERTZ, Guy & Siebentritt, Susanne (2019) Challenge in Cu-rich CuInSe2 thin film solar cells: Defect caused by etching. In: PHYSICAL REVIEW MATERIALS, 3(5) (Art N° 055403).

DOI: 10.1103/PhysRevMaterials.3.055403
Handle: http://hdl.handle.net/1942/30003

Received 00th January 20xx,
Accepted 00th January 20xx

DOI: 10.1039/x0xx00000x

Challenge in Cu-rich $CuInSe_2$ thin film solar cells: Defect caused by etching

Hossam Elanzeery,[a,*] Michele Melchiorre,[a] Mohit Sood,[a] Finn Babbe,[a] Florian Werner,[a] Guy Brammertz,[b,c] and Susanne Siebentritt[a]

a Laboratory for Photovoltaics, Physics and Materials Science Research Unit, University of Luxembourg, Belvaux, L-4422, Luxembourg

b Imec division IMOMEC - partner in Solliance,Wetenschapspark 1, 3590 Diepenbeek, Belgium

c Institute for Material Research (IMO) Hasselt University – partner in Solliance, Wetenschapspark 1, 3590 Diepenbeek, Belgium

*E-mail: Hossam.elanzeery@gmail.com

Thin film solar cells consist of several layers. The interfaces between these layers can provide critical recombination paths and consequently play a vital role in the efficiency of the solar cell. One of the main challenges for polycrystalline semiconductor absorber materials is the absorber/buffer interface. The $Cu(In,Ga)Se_2$ system is particularly interesting in this context, since Cu-rich absorbers are dominated by recombination at the interface, while Cu-poor ones are not. This study unveils the root cause of the challenge in the interface of Cu-rich solar cells in terms of a Se-related defect with an activation energy of 200±20 meV. This defect causes interface recombination and is responsible for the deficiency of open circuit voltage in Cu-rich cells. Moreover, this study demonstrates that the origin of this defect is due to the etching step necessary to remove secondary phases. Post-deposition surface treatments or modified buffer layers are shown to passivate this defect, to reduce interface recombination and to increase the efficiency.

I. INTRODUCTION

Photovoltaics represent one of the promising technologies that are able to provide a renewable source of energy at very low costs with current production of almost 2 % of global electricity [1]. Thin film photovoltaic cells are considered milestones towards achieving high efficient solar cells with lower costs related to their low material and energy consumption, shorter energy payback time and a wide range of possible applications and opportunities [2]. Chalcopyrite copper indium gallium di-selenide (CIGS) represents one of the most promising absorbers for thin film solar cells [3] characterized by their high efficiencies reaching 23.35 % on a laboratory scale [4, 5] and 15.0 % for its ternary compound $CuInSe_2$ (CIS) [6]. CIS and CIGS grown under Cu-excess, referred to as Cu-rich CI(G)S with ([Cu]/[III] ratio > 1, global ratio including secondary Cu selenides) present generally the better semiconductor properties compared to Cu-poor material: larger grains, higher mobility, lower defect densities, better transport properties [7-10] and better collection efficiency [11]. All record solar cells, however, have been prepared from Cu-poor absorbers, because of their higher open-circuit voltage and thus efficiency. The low open-circuit voltage of Cu-rich chalcopyrite solar cells is linked to interface recombination [12]. Nevertheless, it is important to note that a transitory Cu-rich phase during growth has played a significant role in controlling the stress release and the optimization of the absorber quality during growth [3, 13]. State-of-the-art CIGS record cells are based on a 3-stage absorber fabrication process, which involves Cu-poor and Cu-rich phases [14]. Thus, it is important for the thin film community to understand the reason behind the lower efficiencies in Cu-rich thin film solar cells. The lower efficiency in Cu-rich cells compared to Cu-poor ones is due to a strong decrease in the open circuit voltage (V_{OC}). The root cause behind this V_{OC} deficit is due to recombination at the absorber/buffer interface [12, 15, 16]. Interface challenges play a vital role in defining the quality and the efficiency of all solar cells. The interface challenges for polycrystalline semiconductor absorbers like CIGS become even more complex. For Cu-rich thin film solar cells, the root cause of such interface challenges was not clear but has traditionally been attributed to the absence at the surface of the Cu-rich absorbers of an ordered defect compound (ODC) with a higher band gap [12, 17]. However, high-resolution methods like transmission electron microscopy or atom probe tomography generally fail to detect the composition of an ODC at the surface of Cu-poor absorbers [7]. Therefore, we have proposed in the past, tunnel recombination near the interface due to the high absorber doping of Cu-rich material [16, 18]. However, it is difficult to explain the observed dramatic decrease of V_{OC} in Cu-rich solar cells based on a steep band bending alone. Several approaches have been developed to combine Cu-rich absorbers with a Cu-poor surface by implementing different surface treatments [11, 16, 19, 20, 21] that were reported to increase the V_{OC} of Cu-rich cells through the reduction of interface recombination. Recently, it was found that the V_{OC} gap between Cu-rich and Cu-poor cells is related to the bulk recombination and not only to the interface: the quasi-Fermi Level splitting (qFLs) that represents the highest V_{OC} an absorber can achieve, is lower for Cu-rich $Cu(In,Ga)Se_2$ than that of Cu-poor, even before the interface with the buffer is formed [22, 23]. The same study demonstrated a considerably

larger difference between qFLs and V_{OC} in Cu-rich solar cells, indicating, that interface recombination poses an additional loss mechanism in Cu-rich Cu(In,Ga)Se_2. This was confirmed by the investigation of the diode factor in Cu-rich and Cu-poor absorbers and solar cells [24]. In summary: Cu-rich Cu(In,Ga)Se_2 solar cells suffer from interface recombination, but it is not clear, why the buffer-absorber interface is different from the one with Cu-poor absorbers.

According to the phase diagram [25], Cu-rich absorbers are characterized by a stoichiometric chalcopyrite phase with additional copper selenide (Cu_2Se) secondary phases. Etching these conductive secondary phases is mandatory for the electrical performance of such cells [26, 27]. This paper unveils one of the main causes for the dominating interface recombination in Cu-rich solar cells by presenting that this essential etching step is responsible for the formation of defects near the surface acting as recombination centers and deteriorating the performance of such cells. Moreover, this paper highlights the characteristics of such defect and provides means of passivating this defect, restoring part of the lost V_{OC} and leading to an increase in the efficiency of Cu-rich solar cells.

II. RESULTS AND DISCUSSIONS

A. Identification of defects in Cu-rich CIS thin film solar cells

To understand the reason behind the V_{OC} deficit, responsible for the lower efficiency in Cu-rich cells compared to Cu-poor ones, we performed different characterization techniques to identify and analyse defects in Cu-rich CIS that is the ternary end composition of state-of-the-art CIGS thin film solar cells. We performed capacitance measurements as function of frequency and temperature (admittance measurements) in order to identify the main capacitance steps in Cu-rich CIS. These capacitance steps could be either defects or barriers as explained in the experimental section. In this section, we present the main capacitance step in Cu-rich CIS with an activation energy of 200±20 meV, comparing it to Cu-poor values and showing how we identified this 200±20 meV step as a defect and not a barrier.

Admittance measurements (ADM) were performed for Cu-rich and Cu-poor CIS solar cells. The capacitance values are plotted as function of frequency and temperature. The main capacitance step (where a barrier or a defect are likely to respond), is identified by two short dashed lines in all admittance spectra presented in this paper (see Figure 2 for example). The inflection point of these steps are determined from the maxima in the derivative with respect to the log of the frequency as explained in the experimental section below. The values are plotted in an Arrhenius plot. The activation energy of the main capacitance step is then calculated from the slope of the linear fit of this Arrhenius plot [28].

The activation energy of the main capacitance-step revealed from ADM measurements indicated an activation energy of 200±20 meV for the step in Cu-rich cells, while an activation energy of 130±10 meV is deduced in case of Cu-poor CIS cells [29]. It is important to note that this 200±20 meV capacitance step is present in all our Cu-rich CIS cells no matter if we changed the Cu/In ratio or Se flux as reported earlier [30]. The nature of this 200±20 meV step is not a priori clear; whether it is a barrier or a defect and whether it is at the interface or the bulk of the absorber. To unveil the nature of this step, several experiments were performed.

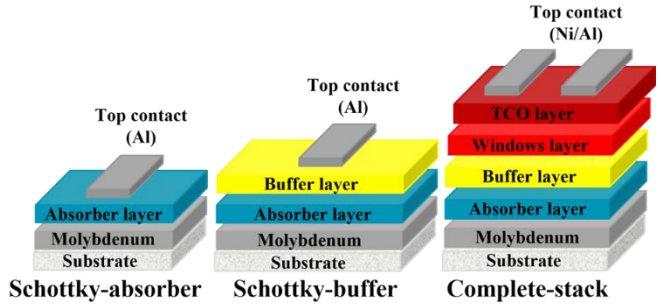

Figure 1: Three different absorber structures: "Schottky-absorber" is the bare absorber covered with an Aluminium (Al) Schottky contact, "Schottky-buffer" is the absorber covered with a CdS buffer layer, then covered with an Aluminium Schottky contact and "complete-stack" is the fully processed solar cell.

Three Cu-rich absorber runs were fabricated with three different Se fluxes (low, medium and high). The pressure of the low Se flux is in the range of $4*10^{-6}$ mbar, medium Se flux is in the range of $1*10^{-5}$ mbar and high Se flux is in the range of $4*10^{-5}$ mbar. Our standard Cu-rich CIS absorber deposition process is performed using the lowest possible Se flux (pressure of $4*10^{-6}$ mbar) as lower Se flux has been reported to be more beneficial for our Cu-rich CIS cells [18] and Se fluxes with pressure lower than $4*10^{-6}$ mbar are not sufficient to form the required CIS phase.

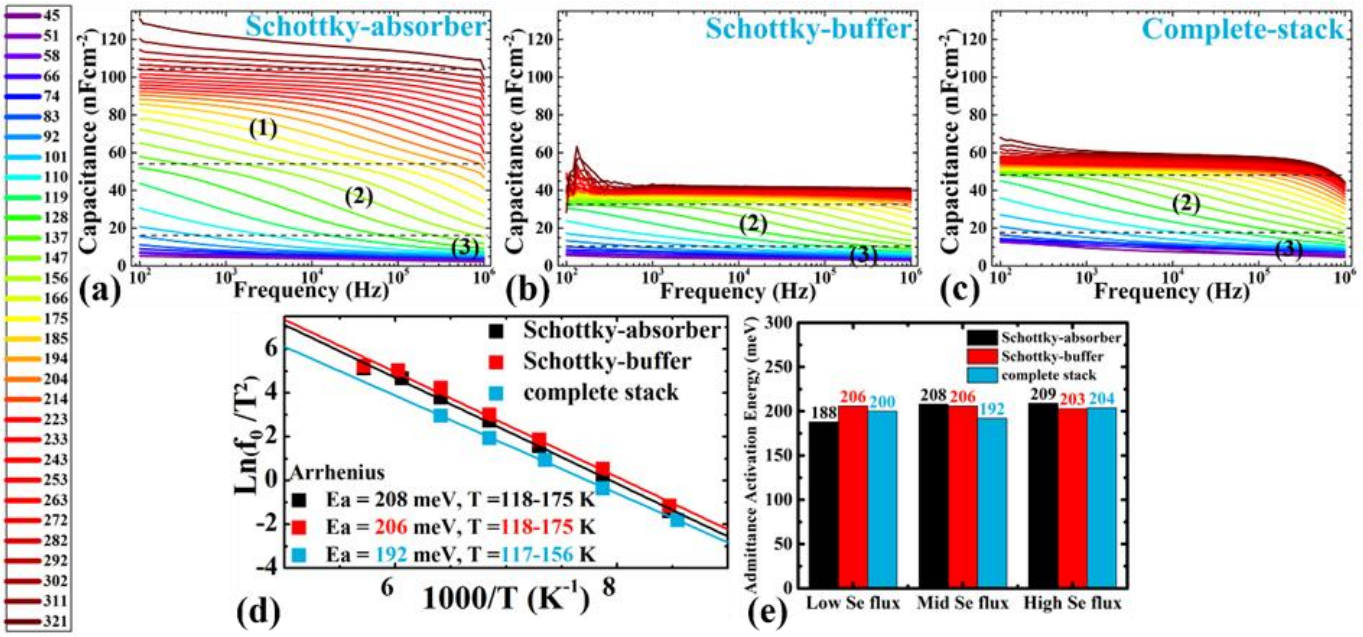

Figure 2: Admittance measurements for: a) Schottky-absorber, b) Schottky-buffer and c) complete-stack of a Cu-rich CIS solar cell grown with a medium Se flux, measured between 320-50 K as indicated by the temperature scale on the left side. d) The Arrhenius plot for Schottky-absorber, Schottky-buffer and complete-stack Cu-rich CIS (a-c) indicating the activation energy of the main capacitance step with values around 200±20 meV for the three samples at the same temperature range (117-175 K). e) Activation energies deduced from admittance measurements for Schottky-absorber, Schottky-buffer and complete-stack for three Cu-rich CIS grown under different Se flux conditions (low, medium and high Se fluxes). The main capacitance step of all samples indicated activation energy of 200±20 meV.

Each absorber fabrication run contains four similar absorbers. One sample was kept for reference and the other three samples were etched using strong potassium cyanide (KCN) etching that is necessary to remove conductive copper selenide secondary phases as explained in the experimental section. The three samples are then completed in three different levels referred to in the text as "Schottky-absorber", "Schottky-buffer" and "complete-stack" as presented in Figure 1 and explained in the experimental section. Aluminium (Al) is deposited on top of the absorber in the case of "Schottky-absorber" and on top of the absorber-buffer surface in case of "Schottky-buffer" to form a Schottky contact [31, 32]. ADM measurements were then performed for the three samples of each of the three absorbers with different Se fluxes with a total of nine samples. The activation energy of the main capacitance step was then deduced from the slope of the Arrhenius plot for all nine samples. The admittance spectra and Arrhenius plots of the three different samples of one of the absorber runs (absorber with medium Se flux) are presented in Figure 2(a-d). The temperature scale of the ADM measurements in Figure 2(a-c) is presented on the left side of Figure 2.

Figure 2(a) represents the ADM spectrum for Cu-rich CIS absorber with Schottky-contact. Three main capacitance steps could be revealed from Figure 2(a) as indicated by the short dashed lines. A high temperature step (represented as step 1) has an activation energy of 280 meV, a medium temperature step (represented as step 2) with an activation energy of 208 meV and a low temperature step (represented as step 3) with an activation energy of 60 meV. After adding a CdS buffer layer in Figure 2(b), the high temperature step disappears leaving only steps 2 and 3 of the medium and low temperatures. The high temperature step (with an activation energy of 280 meV) could be explained as a defect that was caused by the Al contact or passivated by the CdS buffer layer and is not the main focus of this paper. Further processing of the sample in Figure 2(c) reveals that the medium and low temperature steps remain the same with no additional changes. The low temperature step can be attributed to freeze out and could represent the activation energy of the doping defect [10]. Therefore, the main capacitance step for the three samples is the one at intermediate temperatures (step 2) and will be the main focus of this paper. The activation energy of the main capacitance step (medium temperature) for the three samples deduced from the Arrhenius plot in Figure 2(d) indicated an activation energy of 200±20 meV in the same temperature range (117-175 K). The same trend was observed for the other two absorber runs with different Se-fluxes and the activation energies of the main capacitance step for all nine samples are presented in Figure 2(e). Figure 2(e) shows that the activation energy of the main capacitance step for all nine samples is the same with a value of 200±20 meV and in the same temperature range regardless the Se flux used. This capacitance step is present on absorbers with only Schottky contacts and no buffer or window layers indicating that this capacitance step is a property of the absorber. Based on that, this step could be either a bulk defect or a barrier at the back absorber side (Mo/Cu-rich CIS interface).

If this capacitance step was due to a barrier, then the activation energy of the thermally activated series resistance or the forward-bias current should indicate values close to that extracted from admittance measurements (200±20 meV),

otherwise this step would be a defect as explained in the experimental section.

To quantify that, both the series resistance and forward-bias current as function of temperature were deduced from the current-voltage measurements as function of temperature (IVT) performed under dark conditions. The series resistance was extracted from the slope of the IV curves at far forward bias (1.2 V) as function of temperature. At far enough forward bias, the current is limited by either the transport of holes over the back interface barrier between the absorber and the back contact or the transport of electrons at the front interface barrier between the absorber and buffer layers [33] and the series resistance (R_S) is then thermally activated [34]. The activation energy of both the thermally activated series resistance and forward-bias current [35] in Cu-rich CIS solar cells were deduced from the slope of their corresponding Arrhenius plots (Figure S1) indicating values in the range of 100±10 meV and 55±5 meV for the thermally activated series resistance and forward-bias current respectively. These values are much lower than that of the main capacitance step (200±20 meV) in the same temperature range (117-175 K). This means that the main capacitance step in Cu-rich CIS thin film solar cells is indeed a defect in the absorber and not a barrier with an activation energy of 200±20 meV.

B. Means of passivating defects in Cu-rich CIS

As explained above, Cu-rich CIS thin film solar cells suffer from a defect with an activation energy around 200±20 meV. This defect was previously passivated using different types of post-deposition treatments (PDTs) such as an ex-situ KF [11], in-situ KF [20] and In-Se [36] PDTs with a corresponding increase in the V_{OC} after such treatments. After identifying and understanding the nature of this defect as an absorber-related defect, the question arises if we can passivate this defect by modifying the absorber surface using simpler post-deposition treatments than the reported ones or by simply using a modified buffer. In the following two subsections, we will provide means of passivating this 200±20 meV defect using Se-only PDT (sub-section 2.2.1) and using modified buffer layers (sub-section 2.2.2).

1. Passivating defects using Se post-deposition treatment

Se is the common player in all PDTs (In-Se [19, 36], ex-situ KF [11] and in-situ KF [20]) passivating the 200±20 meV defect. It is interesting to discover if a Se-only PDT would also passivate this defect leading to similar improvements to the ones reported in those PDTs or the passivation of the defect was related to In and KF parts of those PDTs.

Four Cu-rich CIS absorbers of the same batch were etched using strong KCN to remove conductive secondary phases as explained earlier. One absorber was used as a reference, ADM measurements were performed on it and the presence of the 200±20 meV defect was confirmed. Then, the remaining three absorbers were all treated with a Se-only PDT, explained in the experimental section and then completed in the same way explained earlier as Schottky-absorber, Schottky-buffer and complete-stack (Figure 1). ADM measurements were performed for the three samples and the three of them indicated an activation energy of 130±10 meV for the main capacitance step as reported [29] and presented in Figure 3. Figure 3(a) represents the admittance spectra for Schottky-absorber treated with Se-only PDT showing three capacitance steps as explained earlier. The high temperature step (step 1) could not be resolved within the measurement range and the low temperature step (step 3) is related to freeze-out with an activation energy of 60 meV. The main capacitance step is again the medium temperature one (step 2) with an activation energy of 122 meV as deduced from the slope of the Arrhenius plot in Figure 3(c). The activation energy of the main capacitance step (130±10 meV) in Schottky absorbers treated with Se-only PDT lies much below that of the untreated Schottky absorbers (200±20 meV) indicating the passivation of this 200±20 meV defect. Moreover, the success of the Se-only PDT in passivating this defect with no buffer layers proves that this defect is related to the absorber and is a Se-related defect. Admittance spectrum for the complete-stack of the Se-treated absorber is presented in Figure 3(b) with the main capacitance step indicated by the two short-dashed lines. The temperature scale for the admittance spectra is presented on the left side of Figure 3. The activation energy of the Se-treated complete-stack sample is extracted from the Arrhenius plot in Figure 3(d) showing a value of 138 meV, which lies in the range of 130±10 meV. The presented activation energies in Figure 3 (c, d) are much less than that of the untreated samples (200±20 meV) confirming that the Se-only PDT is able to passivate this (200±20 meV) defect, indicating that this defect is Se-related.

The disappearance of the 200±20 meV defect using the Se-only PDT is accompanied by an increase in the V_{OC} by around 30 mV, increase in the Fill Factor (FF) by 10 %-absolute and a corresponding increase in the efficiency by 2 %-absolute as presented in Table I. The increase in the V_{OC} as a function of passivating the 200±20 meV defect has been observed after treating Cu-rich CIS with ex-situ KF [11], in-situ KF [20] and In-Se [19, 36] PDTs.

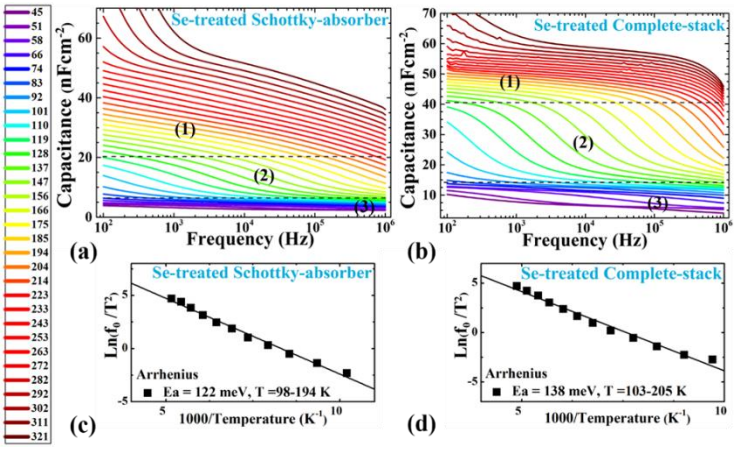

Figure 3: Admittance measurements for a) Schottky-absorber, b) complete-stack of Se-PDT Cu-rich CIS solar cells for temperatures between 320 - 50 K as indicated by the temperature scale on the left. The Arrhenius plot indicates the activation energy of the main capacitance step for c) Schottky-absorber and d) complete-stack Se-PDT Cu-rich CIS solar cells.

Table I: IV parameters extracted from IV measurements under standard test conditions for the average of six solar cells for each of Cu-rich and Se-treated Cu-rich CIS solar cells. Values in brackets represent the IV parameters of the best solar cell.

Sample	Efficiency (%)	FF (%)	V_{OC} (mV)	J_{SC} (mA/cm^2)	R_S (Ω.cm^2)	R_{Sh} (Ω.cm^2)
Cu-rich CIS	7.0 (7.7)	46.8 (50.3)	355 (357)	42.1 (44.3)	0.5 (0.4)	124 (198)
Se-treated Cu-rich CIS	9.2 (9.4)	59.2 (60.6)	382 (385)	40.7 (42.3)	0.4 (0.3)	794 (1153)

2. Passivating defects using modified buffer layers

Passivating the 200±20 meV defect can also be achieved by modifying the buffer layer. From sub-section 2.2.1, it was concluded that the 200±20 meV is a Se-related defect. It was then interesting to discover if using a buffer layer with higher sulphur concentrations would also lead to the passivation of this defect. First, we used a modified CdS buffer layer deposited at EMPA (characterized by its relatively high thiourea concentration and longer durations [37]) as well as a standard Zn(O,S) buffer layer developed in-house with slightly higher thiourea concentrations compared to our standard baseline CdS buffer layer. ADM measurements were performed on Cu-rich CIS etched absorbers with these two buffer layers and Aluminium front contacts forming a Schottky junction. The activation energy for the main capacitance step in both cases showed values of 175±5 meV slightly lower than the 200±20 meV as presented in Figure 4 indicating the passivation of this defect. Motivated by these results, a Zn(O,S) buffer layer with much higher thiourea concentrations compared to our standard Zn(O,S) one (8 times higher thiourea concentration) was deposited on a similar Cu-rich CIS etched absorber. The activation energy deduced from the ADM measurements of this sample with much higher thiourea concentrations showed values of 77±5 meV that is significantly lower than the 175±5 meV with standard lower thiourea concentrations as presented in Figure 4. This means that modified buffer layers with high enough thiourea concentrations (high sulphur contents) are able to passivate the 200±20 meV Se-related defect. Not only that, but interestingly the V_{OC} increased by more than 70 mV for the Cu-rich CIS with Zn(O,S) of high thiourea concentration compared to the same Cu-rich CIS absorber but with standard CdS buffer layer as a consequence of passivating the 200±20 meV defect. The improvement in the V_{OC} (ΔV_{OC}) of Cu-rich CIS cells as a result of passivating the 200±20 meV defect using PDTs with high enough Se and modified buffer layers with high enough S, compared to Cu-rich CIS cells with standard CdS buffer layer, is summarized in Table II. No device was fabricated from the Cu-rich CIS absorber with standard Zn(O,S) buffer layer (Zn(O,S) Low thiourea).

Table II: IV parameters extracted from IV measurements under standard test conditions for the average of six solar cells for each of Cu-rich and Se-treated Cu-rich CIS solar cells. Values in brackets represent the IV parameters of the best solar cell.

Type of treatment	Improvement in V_{OC} (ΔV_{OC})
Ex-situ KF (PDT)	35 mV [11]
In-situ KF (PDT)	60 mV [20]
In-Se (PDT)	100 mV [19]
Se-only (PDT)	30 mV
EMPA CdS (buffer)	35 mV
Zn(O,S) High S (buffer)	70 mV

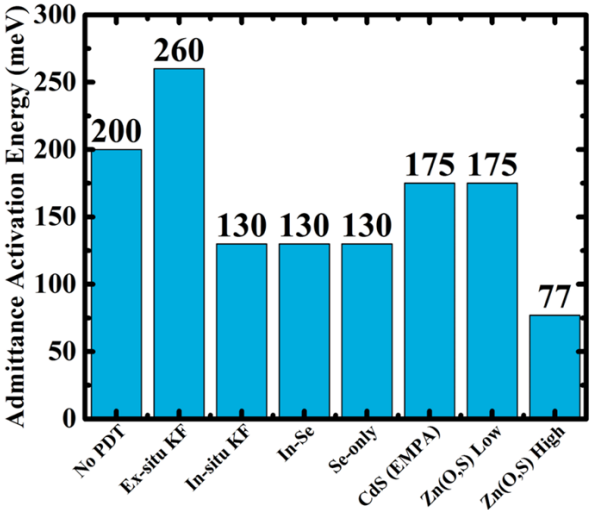

Figure 4: Summary of the activation energies deduced from admittance measurements for different PDTs and buffer layers.

A summary of the activation energies deduced from ADM measurements for different PDTs and buffer layers is presented in Figure 4. It can be concluded from Figure 4 that the 200±20 meV defect can be passivated by ex-situ KF, in-situ KF, In-Se and Se-only PDTs as well as CdS and Zn(O,S) buffer layers with high enough chalcogen concentrations. The high activation energy presented for the ex-situ KF PDT (260±20 meV) has been related to a barrier and not to the 200±20 meV defect. The characteristics of passivating the 200±20 meV defect (explained in Section 2.3) were observed after performing the ex-situ KF PDT as presented in Figure S2.

C. Characteristic of defects in Cu-rich CIS

This section highlights the characteristics of the 200±20 meV defect, its negative effects on the electrical performance of Cu-rich CIS thin film solar cells as well as the positive impacts taking place after passivating this defect.

From the discussions above, it can be concluded that the first characteristic of this 200±20 meV defect is that it is responsible for decreasing the V_{OC} and passivating such defect is always associated with an improvement in the V_{OC} values.

The second characteristic is related to the ADM measurements. Normally, for Cu-rich CIS cells, the admittance derivatives (explained in section 2.1) from which the inflection points of the main capacitance step (200±20 meV) are extracted, are characterized by broad peaks, much broader than those of Cu-poor solar cells (130±10 meV) that are narrow as depicted in Figure 5(a, b). After passivating this 200±20 meV defect, the admittance peaks of the corresponding main capacitance step become narrow again, like Cu-poor. The admittance peaks for the Se-PDT Cu-rich CIS of the same absorber are presented in Figure 5(c) (narrow peaks) as an example for the admittance peak behaviour after the passivation of the 200±20 meV defect from the same absorber.

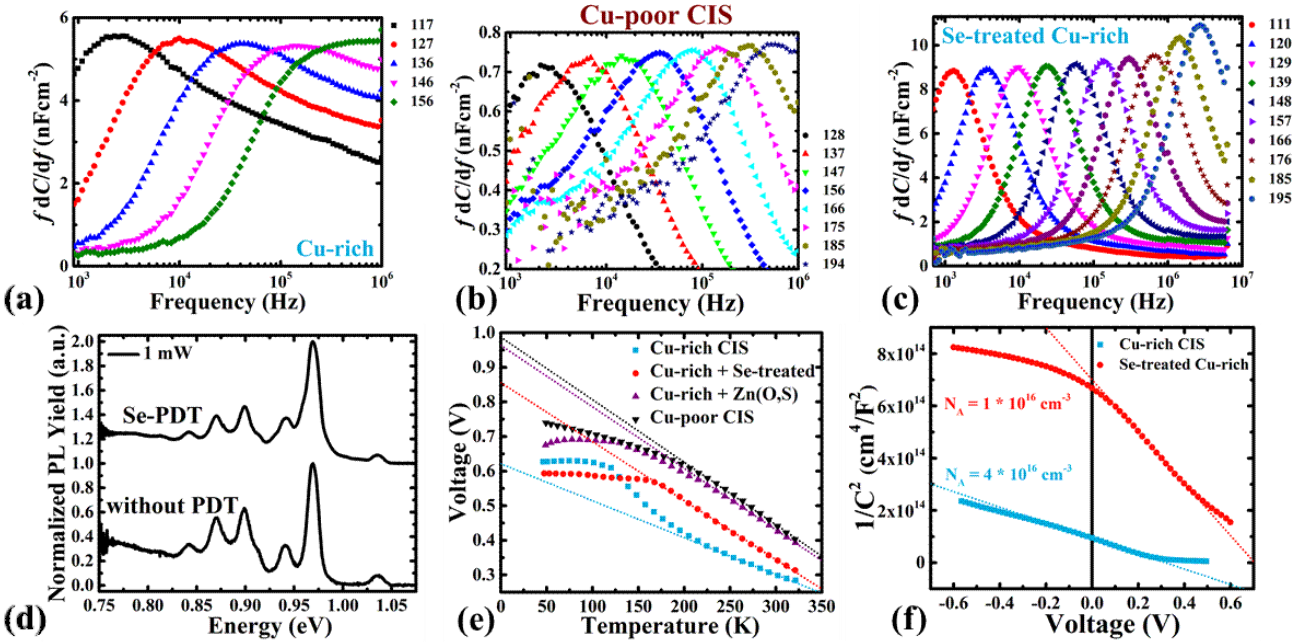

Figure 5: Capacitance derivatives of the main admittance step in a) Cu-rich, b) Cu-poor and c) Cu-rich with Se-PDT. The peaks of the capacitance derivatives are broad in case of Cu-rich and narrow in case of Cu-rich treated with Se-PDT and Cu-poor. The numbers on the right side of each plot indicate the temperature in Kelvin for each of the corresponding presented curves, d) Normalized PL spectra for Cu-rich and Se-treated Cu-rich at a power intensity of 1 mW. The 0.9 eV defect peak is present before and after the Se-PDT, e) Temperature dependence of the open circuit voltage for Cu-poor (black), Cu-rich (blue), Se-treated Cu-rich (red) and Cu-rich with Zn(O,S) of high thiourea concentrations (purple) CIS solar cells. A linear fit at high temperatures (short dotted line) is used to extract the activation energy of the reverse saturation current at zero Kelvin, f) Capacitance-voltage (CV) measurements of an untreated Cu-rich CIS (blue) and a Se-treated Cu-rich CIS (red) solar cells. The apparent doping is extracted from the inverse slope of a linear fit at small forward bias as indicated by the short dotted line.

Moreover, it is interesting to note that the main capacitance step for Cu-rich CIS after a Se-only (Figure 3c), In-Se [36] and in-situ KF [20] PDTs with an activation energy of 130±10 meV occurs in the same temperature range as the main capacitance step before PDTs (200±20 meV step). This means that the broad behaviour of Cu-rich admittance peaks (Figure 5a) reveals the presence of two defects lying in the same temperature range and overlapping each other making their corresponding peaks broad. These two defects are the 200±20 meV and the 130±10 meV defects. Only the one with higher activation energy (200±20 meV) appears in the admittance spectra for untreated Cu-rich CIS while the other is hidden below, but broadens the peak in the derivative curves. After performing a PDT, the 200±20 meV defect is removed and then the other defect with lower activation energy (130±10 meV) appears with a narrow peak (Figure 5c). This hypothesis is also confirmed by the Photoluminescence (PL) measurements presented in Figure 5(d). In Figure 5(d), a PL peak at 0.9 eV is present in Cu-rich CIS spectra before and after the Se-only PDT measured at power intensity of 1 mW. This 0.9 eV peak has been proven to be a defect and reported to be likely the third acceptor defect (A3 defect), in the donor-acceptor pair transition DA3, with an activation energy of 130±10 meV potentially related to Indium vacancy [38]. The defect energy determined from this 0.9 eV PL peak is in excellent agreement with the admittance activation energy (130±10 meV) and proving our hypothesis that the 130±10 meV admittance step is a defect present in Cu-rich CIS solar cells before and after Se-only, In-Se and In-situ KF PDTs.

The third characteristic for the 200±20 meV defect is related to the IVT measurements. The activation energy of the dominant recombination path in thin film solar cells is deduced by extrapolating the temperature dependent V_{OC} to zero Kelvin. If the activation energy is close to the bandgap, then the dominant recombination path is in the bulk of the absorber [39]. Otherwise, if the activation energy at zero Kelvin is less than the bandgap, then the dominant recombination path is at the interface of the absorber [40]. In Cu-rich thin film solar cells, the extrapolated activation energy of the dominant recombination path at zero Kelvin show values lower than the bandgap as presented in Figure 5(e) (blue curve). This indicates that the dominant recombination path is at the interface of the Cu-rich absorbers as reported [11]. In Cu-poor CIS, the corresponding extrapolated activation energy is close to the bandgap indicating that the dominant recombination path is in the bulk of the absorber [11] as presented in Figure 5(e) (black curve). With a Se-PDT (red curve) or Zn(O,S) buffer layer with high thiourea concentrations (purple curve), the extrapolated activation energy at zero Kelvin improved to values closer to the bandgap as presented in Figure 5(e) indicating less influence of the interface recombination in Cu-rich CIS cells. Therefore, it can be concluded that the passivation of the 200±20 meV is always accompanied by an improvement in the activation energy of the dominant recombination path as presented for Se-PDT and Zn(O,S) buffer layer with high thiourea concentrations (Figure 5e) and previously reported with the In-Se [19, 36], ex-situ [11] and in-situ [20] KF PDTs.

The fourth characteristic is related to the slope of the V_{OC} curve as function of temperature in Figure 5(e). In Figure 5(e), the

V_{OC} (T) curve for Cu-rich CIS cells (blue curve) showed two different slopes and not one slope as normally observed for Cu-poor (black curve) before the V_{OC} values saturate at low temperatures. With the Se-PDT (red curve) and Zn(O,S) with high thiourea concentrations (purple curve), one of the two slopes that used to be present for Cu-rich CIS cells disappeared as a result of passivating the 200±20 meV defect, leaving only one slope similar to Cu-poor (black curve) as illustrated in Figure 5(e). The second slope in Cu-rich CIS cells coincides with a strong temperature dependence of the photocurrent at V_{OC}, which makes the model for the activation energy invalid. The relation between the disappearance of the 200±20 meV defect and disappearance of the second slope in the V_{OC} (T) was also reported with ex-situ [11] and in-situ [20] KF PDTs.

The fifth characteristic is linked to the nature of this 200±20 meV defect being an acceptor or donor. Capacitance-voltage (CV) measurements were performed for Cu-rich CIS before and after a Se-PDT (Figure 5f). The inverse slope of the capacitance curves fitted at small forward bias in the Mott-Schottky plot presented in Figure 5(f) was used to extract the apparent doping as explained in the experimental section. In Figure 5(f), Cu-rich CIS has an apparent doping of $4*10^{16}$ cm^{-3} (blue curve) that decreased to $1*10^{16}$ cm^{-3} (red curve) after performing the Se-PDT and passivating the 200±20 meV defect. Similar trends of decreasing the apparent doping were observed after the passivation of the 200±20 meV defect by all other different PDTs such as the in-situ KF [20] and on all three different absorber structures (Schottky-absorber, Schottky-buffer and complete-stack). Based on that, it can be concluded that this defect is an acceptor defect.

We clearly show that the signature of the 200±20 meV defect disappears from the admittance spectra. However, it was shown in the past that a defect signature can vanish without the defect disappearing by a distortion of the band bending: defects seen in a metastable state of the device disappeared in the relaxed state of the device [41, 42]. To check if this could be the case, we placed two devices where we believe the 200±20 meV defect has disappeared (one with high thiourea concentrations and the other with the Se-PDT) into various metastable states and compared admittance and IVT results with the relaxed state. No metastable behaviour could be observed (Figure S3, S4 and S5). Thus, we can conclude that the signature disappears after the PDT because the 200±20 meV defect has in fact been removed from the absorber.

D. Origin of defects in Cu-rich CIS

In the previous sections, we identified a defect, which is only present in Cu-rich CIS thin film solar cells, not in Cu-poor ones. We showed that removing this defect by various PDTs improves the open-circuit voltage. In this section, we will dig more into the possible root causes responsible for the formation of such defects.

Cu-rich CIS by definition is a stoichiometric CIS phase in addition to copper selenide secondary phases according to its phase diagram [25]. Therefore, the origin behind the formation of the Se-related 200±20 meV defect should be related to either a defect present in the stoichiometric CIS phase or related to the additional copper selenide secondary phases and its etching process.

To differentiate between these two potential causes, a stoichiometric CIS absorber was fabricated. This absorber has a Cu/In ratio of 1.0, as measured by EDX, before and after KCN etching. Thus, the sample did not contain any significant amount of secondary Cu selenides phases, even before the etching. This was confirmed by the observation that this absorber resulted in reasonable device with 12.5 % efficiency, without etching it. This device showed the typical characteristics of Cu-rich cells in terms of steep Quantum Efficiency response at long wavelengths [11]. The extrapolated activation energy of the V_{OC} (T) curve of the device made from the unetched absorber at zero Kelvin showed values close to the bandgap of Cu-rich CIS absorbers as presented in Figure 6(a) indicating that the dominant recombination path is in the bulk of the absorber. Moreover, the ADM measurements performed on the stoichiometric absorber without etching showed narrow peaks for its capacitance derivative plot in Figure 6(b) that resembles those of Cu-poor ones, indicating the presence of only one capacitance step. This capacitance step in the stoichiometric absorber is a double-step with activation energies of 100±10 meV and 50±10 meV as presented in the Arrhenius plot of Figure 6c (blue curves). The activation energies of this double-step are close to those reported for high performance Cu-poor CIS cells [43] and could be possibly related to the shallow acceptors: the second acceptor defect (A2 defect), in the donor-acceptor pair transition DA2, (activation energy of 100±10 meV) and the first acceptor defect (A1 defect), in the donor-acceptor pair transition DA1, (activation energy of 50±10 meV) observed by PL measurements [10]. There is no indication for the presence of the 200±20 meV defect. This means that the origin of the 200±20 meV defect lies not in stoichiometric phase itself, leaving the secondary phases and/or the etching process as a possible origin of this defect.

To confirm that and provide a final conclusion statement on this point, the same stoichiometric absorber was subjected to a strong KCN etching in a similar manner to the one performed on Cu-rich CIS absorbers before depositing an Aluminium Schottky contact on the etched stoichiometric absorber [31, 32]. ADM measurements were performed on that sample and the activation energy of the main capacitance step revealed values of 200±20 meV as presented in Figure 6(c) (red curve). The strong KCN etching process was also applied to Cu-poor CIS absorbers and the formation of the 200±20 meV defect was confirmed [29]. Thus, the origin of the 200±20 meV defect is the etching of the absorber, which is necessary in any Cu-rich absorber to remove Cu selenide phases before making it into a device.

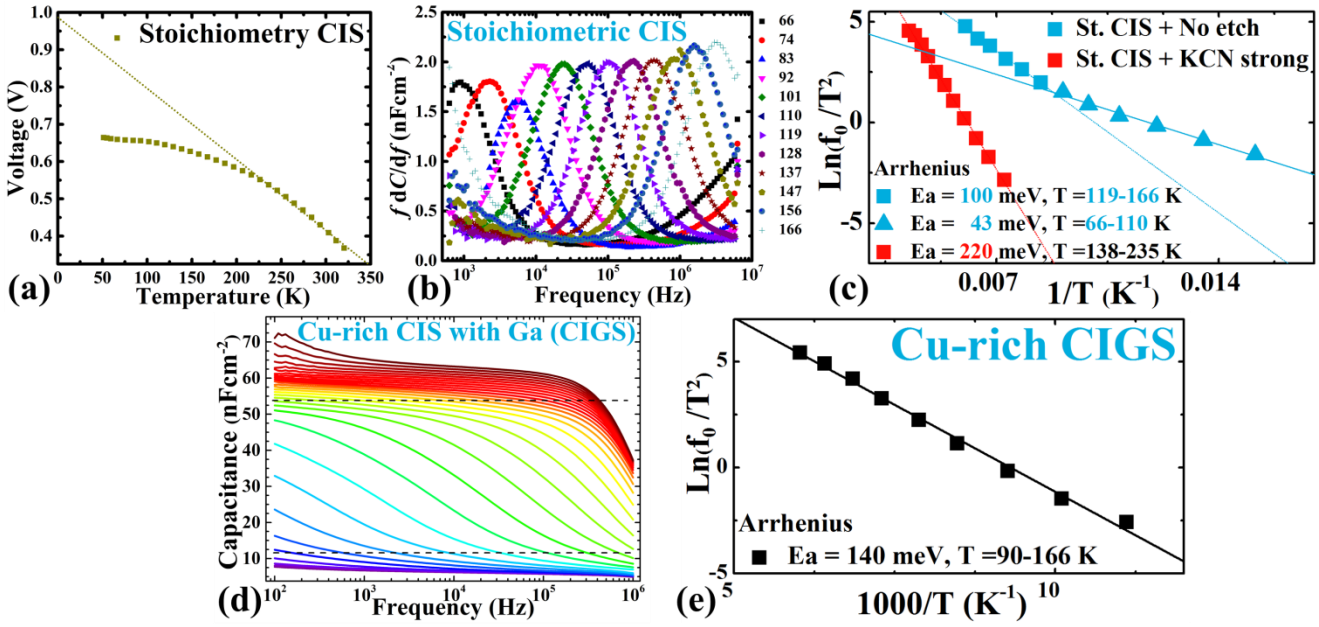

Figure 6: a) Temperature dependence V_{OC} and b) Capacitance derivative plot for un-etched Stoichiometric CIS, c) Arrhenius plot for Stoichiometric CIS absorber with (red) and without (blue) KCN strong etching with their corresponding activation energies of the main capacitance step and temperature ranges. d) Admittance measurements with the temperature scale similar to the ones in Figure 2 and 3, and e) Arrhenius plot for Cu-rich CIGS.

Finally, we would like to mention, that for Cu-rich $Cu(In,Ga)Se_2$, a similar effect of V_{OC} loss compared to Cu-poor cells is observed. This effect is partly healed by using a Ga PDT in the presence of high Se flux as reported [21]. We speculate that the same defect observed in Cu-rich $CuInSe_2$ is formed in Cu-rich $Cu(In,Ga)Se_2$ but is outside the detection limit of our ADM measurements. This defect is passivated in the presence of high Se-flux that restores the lost V_{OC} [21] in a similar manner to Cu-rich $CuInSe_2$. ADM measurements were performed for a Cu-rich $Cu(In,Ga)Se_2$ absorber that was exposed to strong KCN etching as illustrated in Figure 6(d, e). The 200±20 meV defect is not visible and the activation energy of the main capacitance step indicated by the two short dashed lines in Figure 6(d) showed a value of 130±10 meV (Figure 6e) that changes with the addition of Ga corresponding to the third acceptor defect (A3 defect), in the donor-acceptor pair transition DA3, in an excellent agreement with the PL measurements reported [38].

III. EXPERIMENTAL SECTION

A. Synthesis of CI(G)S thin film solar cells

Polycrystalline CIS and CIGS absorbers were fabricated on molybdenum coated soda-lime-glass. Both absorbers were fabricated using physical vapour deposition (PVD) in a Veeco molecular beam epitaxy system. CIS was fabricated using a 1-stage co-evaporation process and $Cu(In,Ga)Se_2$ using a 3-stage process. Cu/III ratio was varied by controlling Cu and In fluxes. Absorbers grown under Cu-excess conditions were fabricated targeting an over-all Cu/III ratio larger than one, referred to in the text as "Cu-rich". Absorbers fabricated with a Cu/III ratio of less than one are referred to in the text as "Cu-poor". Elemental composition of the absorbers is determined through an Oxford instrument energy dispersive x-ray spectroscopy (EDX) with an acceleration voltage of 20 kV. This value represents the average composition of the absorber including Cu_xSe if present. After growth, the absorbers are subjected to a strong etching in a 10 % aqueous solution of potassium cyanide (KCN) for 5 minutes to remove copper selenide secondary phases [26, 27]. For each absorber deposition run, four samples were produced. One absorber is reserved for different characterization techniques. One absorber is used as a bare-absorber, etched and a 3µm Aluminium (Al) layer is deposited using a Ferrotec electron-beam evaporation tool on top of the etched absorber to form a Schottky contact [31, 32]. This type of device is referred to in the text as "Schottky-absorber". A thin CdS buffer layer was deposited on the remaining two etched absorbers through chemical-bath-deposition (CBD). After that, an Aluminium layer is again deposited on top of one of these two absorbers with buffer layers, referred to in the text as "Schottky-buffer". The remaining absorber with CdS buffer layer is then further processed and finished by sputtering both a nominally un-doped and a biased zinc oxide window layers [44] using Aja Orion 8 sputtering tool. Finally, nickel-aluminium contacting grids were evaporated and this device is then referred to in the text as "complete-stack". The different absorber structures are illustrated in Figure 1. A Se post-deposition treatment was developed in the context of this work. Etched absorbers were returned to the PVD and exposed to an annealing step in the presence of Se-only with Se fluxes similar to those used for absorber growth whose pressure is in the range of $4 - 5 * 10^{-6}$ mbar for durations less than 8 minutes and at temperatures between 200 – 250 ^{0}C.

B. Characterization

The electrical parameters were extracted from the current-voltage (IV) measurements performed using a Standard Solar

Simulator, calibrated by a Si reference cell, with a Keithley IV-source-measure-unit. In the set-up used for temperature dependent measurements, a cold mirror halogen lamp was used for illumination with an intensity of 100 mW/cm^2. The activation energy of the dominant recombination channel and the IV-characteristics as function of temperature (IVT) were deduced from the IV characteristics [39] in a temperature range of 320 – 50 K using a CTI-cryogenic closed cycle helium cryostat. The illumination intensity at room temperature of the cold mirror halogen lamp was calibrated to the short circuit current density (J_{SC}) determined from IV under standard test conditions. The capacitance-voltage (CV) as well as the temperature- and frequency-dependent admittance (admittance spectroscopy, ADM) measurements [28] were performed using the same IVT setup with a Precision LCR Meter.

CV measurements are performed to extract the apparent doping from the slope of the Mott-Schottky plot (Figure 5f) at a frequency of 100 KHz fitted at small forward bias (0.03 – 0.2 V) as indicated by the short dotted lines in Figure 5f. This voltage range was chosen as the apparent doping at reverse bias could be influenced by either deep defects that could increase the apparent doping [39] or the doping level that could be depth dependent affected by Cd diffusion and decreasing the apparent doping at the interface [45]. ADM measurements are performed to study the electronic defect states in the semiconductor junction. The finite capture/emission time constants of such a defect level result in distinct steps in the admittance spectrum, which we have marked by the short dashed lines in the experimental capacitance spectra presented in this paper (as in Figure 2). The inflection frequency (f_t) of a capacitance step at a given temperature is determined by the defect response time, and the thermal activation energy of the defect can be obtained from the slope of an Arrhenius plot of the temperature-dependent inflection frequencies. Note that, f_t is commonly scaled with a factor T^{-2} to account for implicit temperature-dependences of the thermal velocity and effective density of states [28, 46, 47]. The presented approach to admittance spectroscopy requires that a given capacitance step is, in fact, caused by a defect level. This is often not the case for typical CIGS solar cells because transport barriers or secondary junctions in the device architecture, for example due to the buffer layer or a Schottky-type back contact, result in identical capacitance steps. When studying defects in CIGS by electronic measurements, it is thus mandatory to exclude effects that might be mistaken for defects by comparing the activation energy of the thermally activated series resistance and forward-bias current as a function of temperature from one side to that extracted from ADM measurements on the other side. If one of the activation energies from series resistance or forward-bias current as function of temperature is in the same range like the activation energy from admittance measurements, then the admittance step is a transport barrier. Otherwise, if both activation energies (series resistance and forward-bias current as function of temperature) are less than that of admittance measurements, then this admittance step shall correspond to a defect [35, 48]. Photoluminescence (PL) measurements were performed using a continuous wave solid state laser diode with a wavelength of 660 nm for optical excitation. The generated PL is collected, guided into a monochromator, spectrally resolved and detected by an InGaAs detector array. The samples are cooled down to 10 K in a liquid Helium flow cryostat for measurements.

IV. CONCLUSION

A defect with an activation energy of 200±20 meV was identified, that appears only in Cu-rich $CuInSe_2$ and not in Cu-poor absorbers. This defect is a Se-related acceptor defect present in the bulk near the surface of Cu-rich CIS absorbers. This defect is the responsible recombination center that shifts the dominant recombination path from the bulk to the interface leading to a decrease in the V_{OC} and the deterioration of the efficiency of such cells. The strong KCN etching step mandatory to remove copper selenide secondary phases was shown to be the origin for the formation of this defect. The same etching step was applied on Cu-poor and stoichiometric CIS absorbers resulting in the formation of the same 200±20 meV defect. The defect can be passivated by any PDT containing Se including Se-only PDT as well as buffer layers with high enough chalcogen concentrations. The passivation of this defect leads to an improvement in the V_{OC}, FF and efficiency of Cu-rich CIS solar cells.

ACKNOWLEDGEMENTS

This contribution has been funded by the Luxembourgish Fonds National de la Recherche (FNR) in the framework of the CURI-K, SURPASS and Massena projects, which are gratefully acknowledged. Christian Andreas and Stephan Bücheler from EMPA are acknowledged for providing CdS buffer layer deposition.

REFERENCES

[1] http://www.goech.at/files/The_7th_CS3_white_paper_12-March_small.pdf (2017)
[2] http://cigs-pv.net/wortpresse/wp-content/uploads/2015/12/CIGS-WhitePaper.pdf (2015)
[3] S. Siebentritt, "Chalcopyrite compound semiconductors for thin film solar cells", *Current Opinion in Green and Sustainable Chemistry* 2017, **4**: 1-7.
[4] http://www.solar-frontier.com/eng/news/2019/0117_press.html (2019)
[5] https://www.pv-magazine.com/2017/12/20/solar-frontier-hits-new-thin-film-cell-efficiency-record/ (2017)
[6] J. AbuShama, R. Noufi, S. Johnston, S. Ward, X. Wu, "Improved performance in $CuInSe_2$ and surface modified $CuGaSe_2$ Solar Cells", *IEEE Photovoltaics Specialists Conference and Exhibition*, 2005: 299-302.
[7] S. Siebentritt, L. Gütay, D. Regesch, Y. Aida, V. Deprédurand, "Why do we make $Cu(In,Ga)Se_2$ solar cells non-stoichiometric?", *Solar Energy Materials and Solar Cells*, 2013, **119**: 18–25.
[8] V. Depredurand, D. Tanaka, Y. Aida, M. Carlberg, N. Fevre, S. Siebentritt, "Current loss due to recombination in Cu-rich $CuInSe_2$ solar cells", *Journal of Applied Physics*, 2014, **115**, 044503.

[9] F. Werner, D. Colombara, M. Melchiorre, N. Valle, B. El Adib, C. Spindler, S. Siebentritt, "Doping mechanism in pure $CuInSe_2$", *Journal of Applied Physics*, 2016, **119**, 173103.
[10] S. Siebentritt, N. Rega, A. Zajogin, M. Ch. Lux-Steiner, "Do we really need another PL study of CuInSe2?", *Phys. Stat. Sol. (c)*, 2004, **1**, 9: 2304-2310.
[11] H. Elanzeery, F. Babbe, M. Melchiorre, A. Zelenina, S. Siebentritt, "Potassium Fluoride Ex-Situ Treatment on Both Cu-Rich and Cu-Poor $CuInSe_2$ Thin Film Solar Cells", *IEEE J. Photovoltaics*, 2017, **7**: 684–689.
[12] M. Turcu, O. Pakma, U. Rau, "Interdependence of absorber composition and recombination mechanism in $Cu(In,Ga)(Se,S)_2$ heterojunction solar cells", *Applied Physics Letters*, 2002, **80**: 2598–2600.
[13] R. Mainz, H. Rodriguez-Alvarez, M. Klaus, D. Thomas, J. Lauche, A. Weber, M. D. Heinemann, S. Brunken, D. Greiner, C. A. Kaufmann, T. Unold, H.-W. Schock, C. Genzel, "Sudden stress relaxation in compound semiconductor thin films triggered by secondary phase segregation", *Phys. Rev. B*, 2015, **92**:155310.
[14] R. Mainz, E. Simsek Sanli, H. Stange, D. Azulay, S. Brunken, D. Greiner, S. Hajaj, M. D. Heinemann, C. A. Kaufmann, M. Klaus, Q. M. Ramasse, H. Rodriguez-Alvarez, A. Weber, I. Balberg, O. Millo, P. A. van Aken, D. Abou-Rasa, "Annihilation of structural defects in chalcogenide absorber films for high-efficiency solar cells", *Energy Environ. Sci.*, 2016, **9**: 1818–1827.
[15] V. Depredurand, Y. Aida, J. Larsen, T. Eisenbarth, A. Majerus, S. Siebentritt, "Surface treatment of CIS solar cells grown under Cu-excess", *37th IEEE Photovoltaic Specialists Conference*, Seattle, WA, 2011: 000337-000342.
[16] Y. Aida, V. Depredurand, J. K. Larsen, H. Arai, D. Tanaka, M. Kurihara, S. Siebentritt, "Cu-rich $CuInSe_2$ solar cells with a Cu-poor surface", *Prog. Photovolt: Res. Appl.*, 2015, **23**: 754–764.
[17] D. Schmid, M. Ruckh, F. Grunwald, HW. Schock, "Chalcopyrite/defect chalcopyrite heterojunctions on the basis of $CuInSe_2$", *Journal of Applied Physics*, 1993, **73**: 2902–2909.
[18] V. Deprédurand, T. Bertram, S. Siebentritt, "Influence of the Se environment on Cu-rich CIS devices", *Physica B*, 2014, **439**: 101–104.
[19] T. Bertram, V. Deprédurand, S. Siebentritt, "In-Se surface treatment of Cu-rich grown $CuInSe_2$", *IEEE 40th Photovoltaic Specialist Conference (PVSC)*, Denver, CO, 2014: 3633-3636.
[20] F. Babbe, H. Elanzeery, M. Melchiorre, A. Zelenina, S. Siebentritt, "Potassium fluoride post deposition treatment with etching step on both Cu rich and Cu poor $CuInSe_2$ thin film solar cells", *Physical Review Materials*, 2018, **2**: 105405.
[21] L. Choubrac, T. Bertram, H. Elanzeery, S. Siebentritt, "$Cu(In,Ga)Se_2$ solar cells with improved current based on surface treated stoichiometric absorbers", *Phys. Status Solidi A*, 2017, **214**, 1: 1600482.
[22] C. Spindler, F. Babbe, M. H. Wolter, F. Ehré, K. Santhosh, P. Hilgert, F. Werner, S. Siebentritt, "Electronic Defects in $Cu(In,Ga)Se_2$ – towards a comprehensive model", in preparation (2018).
[23] F. Babbe, L. Choubrac, S. Siebentritt, "Quasi Fermi level splitting of Cu-rich and Cu-poor $Cu(In,Ga)Se_2$ absorber layers", *Appl. Phys. Lett.*, 2016, **109**: 082105.
[24] F. Babbe, L. Choubrac, S. Siebentritt, "The Optical Diode Ideality Factor Enables Fast Screening of Semiconductors for Solar Cells", *Phys. Status Solidi: Rapid Res. Lett.*, 2018.
[25] T. Gödecke, T. Haalboom, F. Ernst, "Phase Equilibria of Cu-In-Se I. Stable States and Nonequilibrium States of the In_2Se_3-Cu_2Se Subsystem", *Z. Metallkd.*, 2000, **91**: 622-634.
[26] D. Regesch, L. Gütay, J. K. Larsen, V. Deprédurand, D. Tanaka, Y. Aida, S. Siebentritt, "Degradation and passivation of $CuInSe_2$", *Applied Physics Letter*, 2012, **101**.
[27] Y. Hashimoto, N. Kohara, T. Negami, M. Nishitani, T. Wada, "Surface characterization of chemically treated $Cu(In,Ga)Se_2$ Thin Films", Japan Journal of Applied Physics, 1996, 35: 4760-4764.
[28] P. Blood, J. W. Orton, The Electrical Characterization of Semiconductor: Majority Carriers and Electron States, Academic Press, 1992.
[29] D. Colombara, H. Elanzeery, N. Nicoara, D. Sharma, A. Koprek, M. Wolter, N. Valle, O. Bondarchuk, M. Melchiorre, F. Babbe, C. Spindler, O. Cojocaru-Miredin, D. Raabe, P. J. Dale, S. Sadewasser and S. Siebentritt, "Chemical instability of chalcogenide surfaces near phase boundaries", submitted (2019).
[30] T. Bertram, V. Depredurand, S. Siebentritt, "Electrical Characterization of Defects in Cu-Rich Grown $CuInSe_2$ Solar Cells", *IEEE J. Photovoltaics*, 2016, **6**: 546–551.
[31] B. Theys, T. Klinkert, F. Mollica, E. Leite, F. Donsanti, M. Jubault, D. Lincot, "Revisiting Schottky barriers for CIGS solar cells: Electrical characterization of the $Al/Cu(InGa)Se_2$ contact", *Physica status solidi a: applications and material science*, 2016, **213**, 9: 2425-2430.
[32] E. Schlenker, V. Mertens, J. Parisi, R. Reineke-Koch, M. Köntges, "Schottky contact analysis of photovoltaic chalcopyrite thin film absorbers", *Physics Letters A*, 2007, **362**, 2–3, 26: 229-233.
[33] A. Niemegeers, M. Burgelman, "Effects of the Au/CdTe back contact on IV and CV characteristics of Au/CdTe/CdS/TCO solar cells", *Journal of Applied Physics*, 1997, **81**: 2881–2886.
[34] S. M. Sze, K. K. Ng, Physics of Semiconductor Devices, 3rd ed., Wiley India Pvt Limited, 2008.
[35] F. Werner, M. H. Wolter, S. Siebentritt, G. Sozzi, S. D. Napoli, R. Menozzi, P. Jackson, W. Witte, R. Carron, E. Avancini, T. Weiss, S. Buecheler, "Alkali treatments of $Cu(In,Ga)Se_2$ thin-film absorbers and their impact on transport barriers", *Prog Photovolt Res Appl.*, 2018, 1–13.
[36] T. Bertram, Doping, Defects and Solar Cell Performance of Cu-rich Grown $CuInSe_2$, *PhD Thesis*, 2016. Available at http://orbilu.uni.lu/handle/10993/28325
[37] A. Chirila, P. Reinhard, F. Pianezzi, P. Bloesch, A. Uhl, C. Fella, L. Kranz, D. Keller, C. Gretener, H. Hagendorfer, D. Jaeger, R. Erni, S. Nishiwaki, S. Buecheler, A. Tiwari, "Potassium-induced surface modification of $Cu(In,Ga)Se_2$ thin films for high-efficiency solar cells", *Nature Materials*, 2013, **12**: 1107-1111.
[38] F. Babbe, H. Elanzeery, M. H. Wolter, K. Santhosh, S. Siebentritt, "Experimental verification of a third acceptor type defect in $CuInSe_2$ and $Cu(In,Ga)Se_2$ absorber layers", submitted (2019).
[39] D. Abou-Ras, T. Kirchartz, U. Rau, Advanced Characterization Techniques for Thin Film Solar Cells, WILEY-VCH Verlag GmbH & Co. KGaA, 2011.
[40] R. Scheer, "Activation energy of heterojunction diode current in the limit of interface recombination", *Journal of Applied Physics*, 2009, **105**:104505.
[41] P. Zabierowski, U. Rau, M. Igalsona, "Classification of metastabilities in the electrical characteristics of $ZnO/CdS/Cu(In,Ga)Se_2$ solar cells", *Thin Solid Films*, 2001, **387**, 1-2:147-150.
[42] M. Igalson, M. Bodegård, L. Stolt, "Reversible changes of the fill factor in the $ZnO/CdS/Cu(In,Ga)Se_2$ solar cells", *Solar Energy Materials and Solar cells*, 2003, **80**, 2: 195-207.
[43] H. Elanzeery, F. Babbe, M. Melchiorre, F. Werner, S. Siebentritt, "High performance low bandgap thin film solar cells for tandem applications", *Prog. Photovolt. Res. Appl.*, 2018, **26**: 437–442.
[44] M. Hála, H. Kato, M. Algasinger, Y. Inoue, G. Rey, F. Werner, C. Schubbert, T. Dalibor, S. Siebentritt, "Improved environmental stability of highly conductive nominally undoped

ZnO layers suitable for n-type windows in thin film solar cells", *Solar Energy Materials & Solar Cells*, 2017, **161**: 232–239.
[45] F. Werner, T. Bertram, J. Mengozzi, S. Siebentritt, "What is the dopant concentration in polycrystalline thin-film Cu(In, Ga)Se_2?", *Thin Solid Films*, 2017, **633**: 222.
[46] T. Eisenbarth, T. Unold, R. Caballero, C. A. Kaufmann and H.-W. Schock, "Interpretation of admittance, capacitance-voltage, and current-voltage signatures in Cu(In,Ga)Se_2 thin film solar cells", *Journal of Applied Physics*, 2010, **107**: 034509.
[47] F. Werner and S. Siebentritt, "Buffer Layers, Defects, and the Capacitance Step in the Admittance Spectrum of a Thin-Film Solar Cell", *Phys. Rev. Applied American Physical Society*, 2018, **9**: 054047.
[48] C. Schubbert, P. Eraerds, M. Richter, J. Parisi, I. Riedel, T. Dalibor, J. Palm, "A simulation study on the impact of band gap profile variations and secondary barriers on the temperature behavior, performance ratio, and energy yield of Cu(In,Ga)$(Se,S)_2$ solar cells", *physica status solidi (a)*, 2015, **212**: 336-347.